

## MgB<sub>2</sub> Superconducting Whiskers Synthesized by Using the Hybrid Physical–Chemical Vapor Deposition

Yazhou Wang, Chenggang Zhuang, Jingyun Gao, Xudong Shan, Jingmin Zhang, Zhimin Liao, Hongjun Xu, Dapeng Yu,\* and Qingrong Feng\*

State Key Laboratory for Mesoscopic Physics, Department of Physics, Peking University, Beijing 100871, P. R. China

Received November 19, 2008; E-mail: qrfeng@pku.edu.cn; yudp@pku.edu.cn

Since the discovery of superconductivity in MgB<sub>2</sub> in 2001,<sup>1</sup> tremendous research activities have been stimulated. Both understanding the basic properties and searching for mass production toward large scale applications are highly important for the study of MgB<sub>2</sub>. MgB<sub>2</sub> has a remarkably high  $T_c(0)$  of  $\sim 39$  K, a relatively high coherence length<sup>2</sup> of  $\sim 5$  nm compared with the high critical current density up to  $1 \times 10^8$  A/cm<sup>2</sup> at 2 K and self-field,<sup>3</sup> and a larger energy gap<sup>4</sup> without a weak link between grain boundaries.<sup>5</sup> All these advantages make it a promising candidate for applications in superconducting devices operating in the temperature range 4–20 K. In the past few years, research and development of MgB<sub>2</sub> have been rapidly progressing. Up to now, study of the MgB<sub>2</sub> and its derivative has been mainly focused on the bulk,<sup>6,7</sup> thin films,<sup>8,9</sup> wires,<sup>10,11</sup> and only a few reports on the synthesis of MgB<sub>2</sub> nanowires and nanoparticles.<sup>12–15</sup> However, little has been reported on the synthesis of MgB<sub>2</sub> whiskers. Superconducting nanowires and other 1D nanostructure can be used as the ideal low-dissipated interconnections in superconducting devices; thus it is desirable to grow MgB<sub>2</sub> whiskers and other nanostructures on a substrate. Fabrication and investigations of the nanodevices based on MgB<sub>2</sub> provide a fundamental understanding of the effect of dimensionality and size effects on superconductivity. In this paper, we report on the synthesis of the MgB<sub>2</sub> superconducting nanowhiskers on copper and other substrates (see Figure S1 in the Supporting Information) by using the hybrid physical–chemical vapor deposition (HPCVD) technique. The HPCVD method can provide a sufficiently high Mg vapor pressure for the thermodynamic phase stability of MgB<sub>2</sub> at elevated temperatures, which is the most effective method for MgB<sub>2</sub> synthesis. The MgB<sub>2</sub> whiskers have a hexagonal conelike morphology and a length of  $\sim 4$   $\mu\text{m}$ . The onset transition temperature is  $\sim 39$  K.

The HPCVD growth method used in this experiment is successful in making high quality MgB<sub>2</sub> film.<sup>16,17</sup> The principle of the HPCVD and the scheme of the setup were described elsewhere.<sup>16</sup> A quartz chamber with induction heating and a stainless steel chamber with resistivity heating are the two mostly employed HPCVD setups, and a quartz reactor is used.<sup>16</sup> Essentially, the substrate circled with the Mg ingots was placed on a stainless steel susceptor and heated to a desired deposition temperature inductively by an rf-generator. Boron decomposed from the B<sub>2</sub>H<sub>6</sub> reacted with sufficient Mg vapor near the substrate and formed MgB<sub>2</sub>. During the entire reaction process, pure H<sub>2</sub> was introduced as ambient gas. The sample was deposited at 650 °C for 4 min, and the surface of the copper substrate was polished using a very fine sand grinding paper. The ambient pressure in the reacting chamber was maintained at  $\sim 25$  KPa. The flow rates of B<sub>2</sub>H<sub>6</sub> (with concentration of 25% in hydrogen) and H<sub>2</sub> were 25 and 100 sccm, respectively.

After the deposition, MgB<sub>2</sub> nanostructures can be observed with the naked eye at the edge of the film on the substrates. The

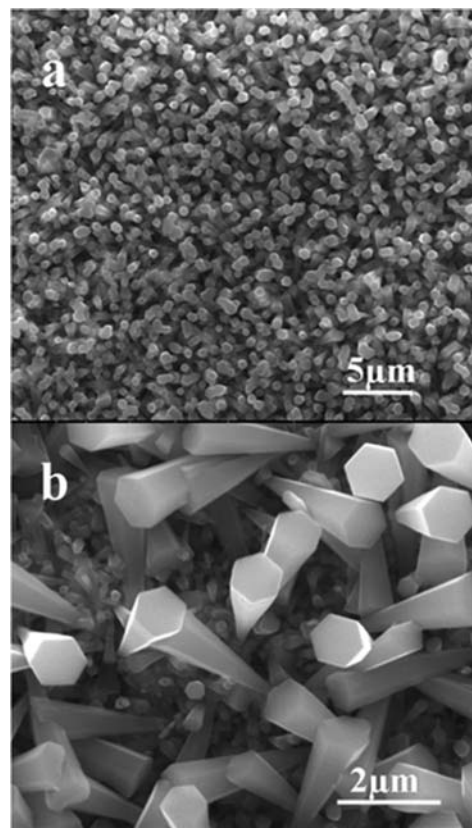


**Figure 1.** (a) Low and (b) high magnification SEM images of the MgB<sub>2</sub> whiskers grown on the copper substrate.

morphologies of the whiskers were analyzed using a scanning electron microscope (SEM, QUANTA 200 FEG) (Figure 1). The low and high magnification SEM images of the whiskers are shown in (a) and (b), respectively, indicating that the whiskers have an average length of  $\sim 4$   $\mu\text{m}$ . The morphology analysis reveals that the whiskers have a hexagonal cone shape and the top diameter is  $\sim 1$   $\mu\text{m}$  while the bottom is  $\sim 200$  nm. It is noted that there also exist many thin whiskers at the bottom of the large ones, whose length is in the range 20 nm to 1  $\mu\text{m}$ .

The microstructure of individual MgB<sub>2</sub> whiskers was investigated by transmission electron microscopy (TEM, TECNAI F30). A bright-field TEM image of a single MgB<sub>2</sub> whisker is shown in Figure 2a. The incident electron beam is parallel to the  $[\bar{1} 2 \bar{1} 0]$  zone axis. The corresponding selected area electron diffraction (SAED) pattern taken from the MgB<sub>2</sub> whisker reveals that the whisker has a hexagonal single crystal structure. The electron diffraction pattern in the inset was indexed with the indices (10

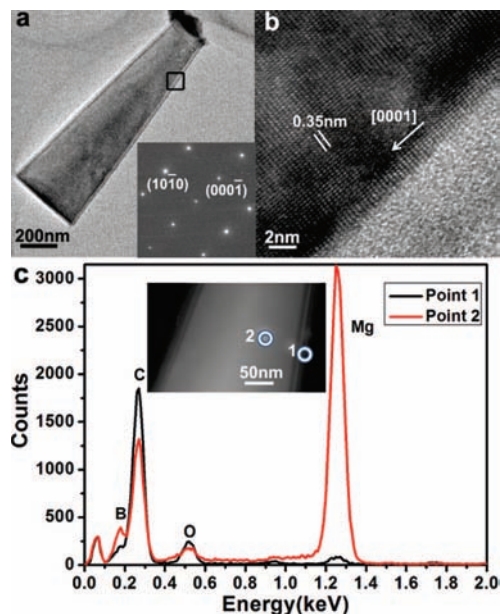


**Figure 2.** (a) TEM image of the  $\text{MgB}_2$  whisker. The inset is the SAED pattern of the  $\text{MgB}_2$  whisker. (b) High resolution TEM image of the  $\text{MgB}_2$  whisker. (c) EDS analysis on individual  $\text{MgB}_2$  whisker. The black curve is taken from point 1 and the red one from point 2, revealing that the sheathing layer consists of  $\text{Mg}_x\text{B}_y\text{O}_z$ .

$\bar{1}0$ ) and  $(000\bar{1})$ . The high resolution TEM image taken from the same  $\text{MgB}_2$  whisker indicates that the whisker is grown along the  $[0001]$   $c$ -axis and the lattice spacing is  $\sim 0.35$  nm, corresponding to the  $(0001)$  plane of the  $\text{MgB}_2$  (Figure 2b). The TEM image also shows that the whisker has an amorphous sheathing layer  $\sim 10$  nm in thickness. Compositional analysis on individual  $\text{MgB}_2$  whiskers was conducted by using energy dispersive spectroscopy (EDS) with TEM. The EDS spectra (Figure 2c) were collected from two selected points: the outer sheathing layer and the body of the whisker. Magnesium, boron, and oxygen were detected at both points. The ratio of oxygen to magnesium in point 1 is much higher than that in point 2, revealing that the sheathing layer consists of Mg and O with detected B. It is noted that, according to the above EDS results, the ratio of B over O in the body is much higher than that in the sheathing layer. Therefore, we can conclude that the amorphous sheathing layer of the whiskers is composed of  $\text{Mg}_x\text{B}_y\text{O}_z$ .

The whiskers were collected from the surface of the substrate, and their magnetic properties were measured with the magnetic property measurement system (MPMS, Quantum Design). The magnetization as a function of temperature ( $M$ - $T$  curve) reveals that the onset superconducting temperature is  $\sim 39$  K (Figure 3), which is higher than the superconducting transition temperature of the bulk  $\text{MgB}_2$  film on copper substrates.<sup>18</sup> This may be due to the fact that the  $\text{MgB}_2$  whisker is of a single crystalline structure.

The growth mechanism of the  $\text{MgB}_2$  whiskers is of great interest and deserves being discussed in detail. Since the  $\text{MgB}_2$  whiskers can grow on different substrates like Cu, Mg, and stainless steel, the growth of  $\text{MgB}_2$  may not need a catalyst. We believe the possible mechanism is dominated by self-seed growth. When the Mg ingots were heated to  $650$  °C, Mg melted and vaporized. Then,  $\text{B}_2\text{H}_6$  decomposed and B atoms reacted with Mg vapor; as a result, a layer of dense  $\text{MgB}_2$  film was formed on the substrate. This film can act as a seed layer, which can provide favorable nucleation sites (Figure S2). Due to the anisotropy growth rate,  $\text{MgB}_2$  whiskers will grow on such a seed layer as cone-shaped whiskers close to

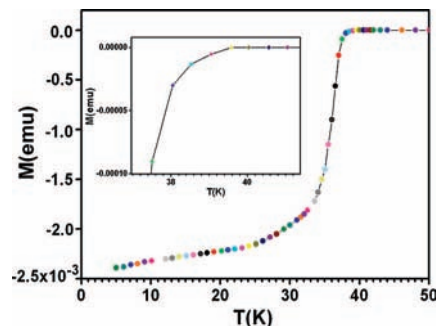


**Figure 3.**  $M$ - $T$  curve of the  $\text{MgB}_2$  whiskers measured under a magnetic field of 50 Oe. The inset shows the onset transition temperature  $\sim 39$  K.

the Mg source where the Mg vapor concentration is higher. The above suggestion was confirmed by the fact that many smaller whiskers were observed to grow directly from the body of bigger ones, with no catalysts but the whisker itself, which proves that the mechanism of the  $\text{MgB}_2$  whiskers is by self-seeded growth. A similar mechanism was also used to explain the growth of ZnO whiskers or nanowires without catalysts.<sup>19,20</sup>

In summary, by using the HPCVD technique, we demonstrated the superconducting  $\text{MgB}_2$  whiskers synthesized on copper substrates. The cone-shaped  $\text{MgB}_2$  whiskers have a hexagonal shape and grow along the  $[0001]$  direction with a single-crystal structure. An onset transition temperature of 39 K is observed. The possible mechanism is by self-seeded growth.

**Acknowledgment.** This work is supported by NSFC (50572001, 10804002, 90606023, 20731160012, 10804003), 973 program (2007CB936202/04, 2009CB623703, MOST) and NSFC/RGC (N HKUST615/06), and the National Foundation for Fostering Talents of Basic Science under Grant No. J0630311.

**Supporting Information Available:** SEM images with full list of authors for refs 5 and 17. This material is available free of charge via the Internet at <http://pubs.acs.org>.

## References

- (1) Nagamatsu, J.; Nakagawa, N.; Muranaka, T.; Zenitani, Y.; Akimitsu, J. *Nature* **2001**, *410*, 63.
- (2) Finnermore, D. K.; Ostenson, J. E.; Budko, S. L.; Lapertot, G.; Canfield, P. C. *Phys. Rev. Lett.* **2001**, *86*, 2420.
- (3) Zhuang, C. G.; Meng, S.; Zhang, C. Y.; Feng, Q. R.; Gan, Z. Z.; Yang, H.; Jia, Y.; Wen, H. H.; Xi, X. X. *J. Appl. Phys.* **2008**, *104*, 013924.
- (4) Tsuda, S.; Yokoya, T.; Kiss, T.; Takano, Y.; Togano, K.; Kito, H.; Lhara, H.; Shin, S. *Phys. Rev. Lett.* **2001**, *87*, 177006.
- (5) Larbalestier, D. C.; et al. *Nature* **2001**, *410*, 186.
- (6) Badr, M. H.; Ng, K. W. *Supercond. Sci. Technol.* **2003**, *16*, 668.
- (7) Lan, M. D.; Tasi, P. L.; Chang, Y. L.; Cheng, J. J. *Solid State Commun.* **2002**, *121*, 575.
- (8) Kang, W. N.; Kim, H. J.; Choi, E. M.; Jung, C. U.; Lee, S. I. *Science* **2001**, *292*, 1521.
- (9) Eom, C. B.; Lee, M. K.; Choi, J. H.; Belenky, L. J. *Nature* **2001**, *411*, 558.
- (10) Jin, S.; Mavoori, H.; Bower, C.; van Dover, R. B. *Nature* **2001**, *411*, 563.
- (11) Canfield, P. C.; Finnermore, D. F.; Bud'ko, S. L.; Ostenson, J. E.; Lapertot, G.; Cunningham, C. E.; Petrovic, C. *Phys. Rev. Lett.* **2001**, *86*, 2423.
- (12) Wu, Y.; Messer, B.; Yang, P. *Adv. Mater.* **2001**, *13*, 1487.
- (13) Cao, L.; Zang, Z.; Wen, H.; Wang, W. *Appl. Phys. Lett.* **2005**, *86*, 123113.
- (14) Nath, M.; Parkinson, B. A. *J. Am. Chem. Soc.* **2007**, *129*, 11302.
- (15) Nath, M.; Parkinson, B. A. *Adv. Mater.* **2006**, *18*, 1865.
- (16) Zeng, X.; Pogrebnjakov, A. V.; Kotcharov, A.; Jones, J. E.; Xi, X. X.; Lysczek, E. M.; Redwing, J. M.; Xu, S.; Li, Q.; Lettieri, J.; Schlom, D. G.; Tian, W.; Pan, X.; Liu, Z. K. *Nat. Mater.* **2002**, *11*, 35.
- (17) Xi, X. X.; et al. *Physica C* **2007**, *456*, 22.
- (18) Li, F.; Guo, T.; Zhang, K. C.; Chen, L.; Chen, C. P.; Feng, Q. R. *Supercond. Sci. Technol.* **2006**, *19*, 1196.
- (19) Greene, L. E.; Law, M.; Tan, D. H.; Montano, M.; Goldberger, J.; Somorjai, G.; Yang, P. D. *Nano Lett.* **2005**, *7*, 1231.
- (20) Ghosh, R.; Dutta, M.; Basak, D. *Appl. Phys. Lett.* **2007**, *91*, 073108.

JA8087828